Adsorption and Catalytic Oxidation of Gaseous Elemental Mercury in Flue Gas over MnO_x/Alumina

Shaohua Qiao, Jie Chen, Jianfeng Li, Zan Qu, Ping Liu, Naiqiang Yan,* and Jinping Jia

School of Environmental Science & Engineering, Shanghai Jiao Tong University, Shanghai 200240, P. R. China

MnO_x/Al_2O_3 catalysts (i.e., impregnating manganese oxide on alumina) were employed to remove elemental mercury (Hg^0) from flue gas. MnO_x/Al_2O_3 was found to have significant adsorption performance on capturing Hg^0 in the absence of hydrogen chloride (HCl), and its favorable adsorption temperature was about 600 K. However, the catalytic oxidation of Hg^0 became dominant when HCl or chlorine (Cl_2) was present in flue gas, and the removal efficiency of Hg^0 was up to 90% with 20 ppm of HCl or 2 ppm of Cl_2. In addition, the catalysts with adsorbed mercury could be chemically regenerated by rinsing with HCl gas to strip off the adsorbed mercury in the form of $HgCl_2$. Sulfur dioxide displayed inhibition to the adsorption of Hg^0 on the catalysts, but the inhibition was less to the catalytic oxidation of Hg^0, especially in the presence of Cl_2. The analysis results of XPS and pyrolysis−AAS indicated that the adsorbed mercury was mainly in the forms of mercuric oxide (HgO) and the weakly bonded speciation, and the ratio of them varied with the adsorption amount and manganese content on catalysts. The multifunctional performances of MnO_x/Al_2O_3 on the removal of Hg^0 appeared to be promising in the industrial applications.

1. Introduction

Mercury has become the leading concern among the air toxicants because of its high volatility, long persistence, and strong bioaccumulation properties.[1] It has been listed as a hazardous and toxic pollutant under Title III of the 1990 Clean Air Act Amendments (CAAA) in the United States. Coal combustion is a major source of anthropogenic emissions of mercury.[2] For example, the mercury emissions from coal combustion increased from 202 tons in 1995 to 257 tons in 2003 in China, with an annual growth rate of 3.0% on average.[3,4] Increasing awareness of the mercury emissions from coal-fired flue gas has led to many efforts to develop strategies and technologies for the reduction of mercury. The U.S. EPA's Clean Air Mercury Rule (CAMR) of 2005 mandated a transition to capped mercury emissions in the next decade. It is possible that more stringent regulations may replace CAMR, which was vacated by the District of Columbia Court of Appeals in 2008.

Mercury in flue gas can be emitted in three forms: oxidized mercury (Hg^{2+}), elemental mercury (Hg^0), and the particulate phase (Hg^p).[5] Among these forms, Hg^0 is the most difficult one to be captured because of its high volatility and low solubility in water. The existing air pollution control devices (APCDs) have demonstrated certain cobenefits of mercury control. The electrostatics precipitators (ESPs) and the fabric filters (FF) are effective to remove Hg^p; meanwhile, the flue gas desulfurization (FGD) systems can capture more than 80% of Hg^{2+}.[6,7]The catalysts employed in the selective catalytic reduction (SCR) of nitrogen oxides have also been proven to facilitate the heterogeneous oxidation of Hg^0 to Hg^{2+}, which can be effectively captured by FGD downstream.[8,9] However, the oxidation extent of Hg^0 across SCR mainly depends on chloride concentration in different coals. Thirty to ninety-eight percent oxidation of Hg^0 was obtained when burning bituminous coal, while the lower chloride content in subbituminous coal greatly reduced the oxidation efficiency to 0−26%.[10,11]

Recently, the catalysts employing manganese oxides as the active ingredient have attracted substantial attention in SCR because of their high catalytic activities under a wide range of temperatures. Among the new developing SCR catalysts, manganese oxides supported on Al_2O_3, NaY, TiO_2, or active carbon have been investigated intensively.[12−14] However, the roles of such catalysts on the catalytic oxidation and the removal of Hg^0 have not been well understood yet.

In this study, the catalysts prepared by impregnating manganese oxide on alumina were studied with respect to their adsorption and catalytic oxidation performance on Hg^0 in the simulated flue gas. Meanwhile, the essential analysis and characterization of catalysts have been conducted to reveal the possible mechanism of Hg^0 adsorption and conversion on the catalysts.

2. Experimental Section

2.1. Apparatus. The apparatuses used in the study of Hg^0 adsorption and catalytic oxidation are shown in Figure 1, including a mercury generator, a packed-bed catalytic reactor, a temperature-controlled furnace, and an online mercury analyzer. The self-made Hg^0 generator consisted of a mercury permeation tube (with 0.8 cm^2 of the cation-permeable membrane) placed at 60 °C in a constant temperature system. The flow rate of each gas stream was accurately controlled by a mass flow controller (MFC) before entering the reactor (10 mm of the inner diameter and 40 cm in length, quartz). The packed volume of the catalysts was 3.2 mL. Hg^0 concentration was online monitored by a cold vapor atomic adsorption spectrophotometry mercury analyzer (SG-921, Jiangfen Ltd.). Hg^{2+} in the outlet was collected with three impingers containing aqueous solution of potassium chloride discontinuously and analyzed by an RA-915+ Mercury Analyzer (Lumex Ltd., Russia) subsequently.

2.2. Materials. Inert alumina (α-Al_2O_3) and active alumina (γ-Al_2O_3) were selected as the catalyst carriers. Both of them were pellets with diameters of 2 ± 0.5 mm, and the BET surface areas were 0.4 and 303 $m^2\ g^{-1}$, respectively.

MnO_x/alumina catalysts were prepared by wet impregnation methods with manganous nitrate (Sino-pharm Chemical Reagent) as precursor. The dried carriers were impregnated in the

* To whom correspondence should be addressed. Tel.: +86 21 54745591. Fax: +86 21 54745591. E-mail: nqyan@sjtu.edu.cn.

10.1021/ie801478w CCC: $40.75
Published on Web 02/25/2009

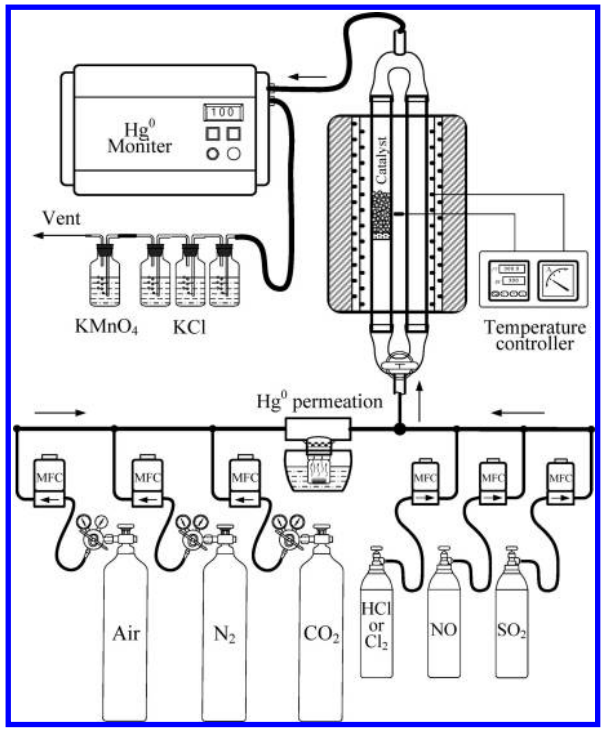

Figure 1. Schematic diagram of the experimental setup for the tests of Hg^0 adsorption and catalytic oxidation.

demanded concentration of $Mn(NO_3)_2$ solution. After the impregnation, the carriers were dried at 333 K for 12 h and then calcined in the air at 573 K for 1 h and at 673 K for 3 h. Since α-Al_2O_3 was less porous, the maximum content of manganese (Mn) was kept at 1.0 wt % to avoid the fragile shell of MnO_x that was easy to fall off. However, the Mn content on γ-Al_2O_3 can reach 8.0 wt % without visible shell layer (mainly dispersed into the porosities on the carrier). Therefore, the loaded Mn contents of 1%, 2.5%, 5%, and 8% were prepared for the MnO_x/γ-Al_2O_3 catalysts.

The gases of sulfur dioxide (SO_2) (100%), nitrogen oxide (NO) (10%), hydrogen chloride (HCl) (5000 ppm), and Cl_2 (200 ppm) were produced by Dalian Special Gas Co. The compressed air and nitrogen in gas cylinders were used as the balance gases to prepare the simulated flue gases. All chemicals were of analytical grades.

2.3. Test Conditions. In each experiment, 3.2 mL of catalysts (corresponding to 3.6 g of MnO_x/α-Al_2O_3 or 2.4 g of MnO_x/γ-Al_2O_3) were filled in the reactor and pretreated at 573 K for 1 h to get rid of the adsorbed water vapor and other impurities. Subsequently, the simulated flue gas with 20 ppbv of Hg^0 vapor was switched into the reactor at the desired temperature (373−773 K). The mercury recovery ratio across the reactor was checked with the blank α-Al_2O_3 and γ-Al_2O_3 as references, which was about 98%. Then the catalysts were exposed to the gas stream at the flow rate of 100 L/h for several days (~100 h) until the Hg^0 concentration in the outlet reached 90% of that in the inlet, where the space velocity was 31 250 h^{-1}. According to our preliminary tests, the effects of NO and CO_2 on the catalysis were insignificant, and the water vapor has no obvious effect ranging from 0 to 5%. However, sulfur dioxide (SO_2) showed significant effect on the catalysis. Therefore, the impact of SO_2 on the oxidation of Hg^0 was investigated by adding 200−2000 ppmv of SO_2 into the simulated gases.

The mercury adsorbed on the catalysts was determined by an RA-915$^+$ Mercury Analyzer (Lumex Ltd., Russia) equipped with a pyrolysis unit (RP-91C). The RP-91C unit enables the direct determination of adsorbent mercury on solid samples by a pyrolysis technique instead of chemical pretreatment. In addition, the speciation of adsorbent mercury could be preliminarily determined from the mercury pyrolysis curves integrated with the common chemical identification.

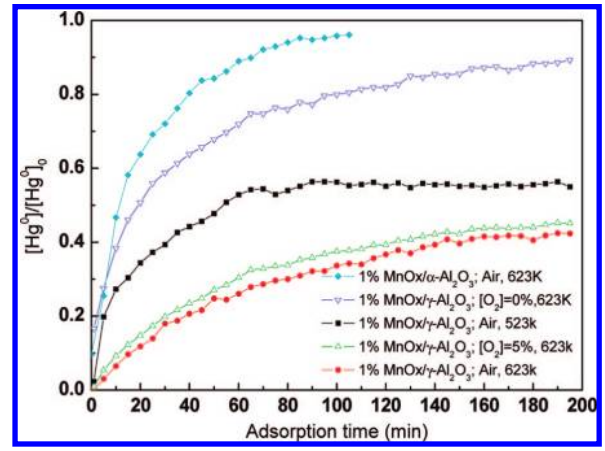

Figure 2. Breakthrough curves of elemental mercury across the catalysts. Air was used as the balance gas, and the packed volume of the catalyst was 3.2 mL (corresponding to 3.6 g of MnO_x/α-Al_2O_3 or 2.4 g of MnO_x/γ-Al_2O_3) if not indicated particularly.

X-ray photoelectron spectroscopy (XPS, PHI-5000C ESCA) was used to determine the binding energies of Mn 2p, O 1s, and Hg 4f with Mg Kα radiation ($h\nu$ = 1253.6 eV). The C1s line at 284.6 eV was taken as a reference for the binding energy calibration.

3. Results and Discussions

3.1. Hg^0 Adsorption on the Catalysts in the Absence of HCl. Figure 2 shows the time-dependent breakthrough curves of Hg^0 across the reactors with catalysts under various conditions. The removal efficiency of Hg^0 after 2 h adsorption (η_{2h}) shown in eq 1 and the adsorption capacity at 90% breakthrough point (the outlet Hg^0 concentration equaling 90% of that in the inlet, $Q_{90\%}$) were employed as the parameters for the comparison among the catalysts under various conditions.

$$\eta_{2h} = 1 - [Hg^0]_i/[Hg^0]_0 \quad (1)$$

where $[Hg^0]_0$ is the inlet Hg^0 concentration and $[Hg^0]_i$ denotes the outlet Hg^0 concentration at 2 h of adsorption.

The Effect of the Carrier Surface and Oxygen on Hg^0 Adsorption. It can be observed from Figure 2 that the adsorptions of Hg^0 on the catalysts with α-Al_2O_3 and γ-Al_2O_3 as the carriers were significantly different even with the same Mn content loaded (1.0 wt %). The half-breakthrough time (the time when the outlet Hg^0 concentration is equal to 50% of that in the inlet, $t_{1/2}$) was only 15 min for the reactor filled with MnO_x/α-Al_2O_3, but it was more than 200 min for that with MnO_x/γ-Al_2O_3. In addition, the Hg^0 adsorption capacity of the two catalysts at the point of 90% breakthrough ($Q_{90\%}$) at 623 K was 1.6 and 75 μg/g, respectively. The difference can be explained by the surface areas. MnO_x could be well dispersed on the porous surface of γ-Al_2O_3, which is helpful to yield more active sites on catalysts for Hg^0 adsorption. However, MnO_x tends to form a dense shell on α-Al_2O_3, and most of the MnO_x in the deep layer is inaccessible to adsorb Hg^0 because of the higher gas diffusion resistance.

Figure 2 also shows the effect of oxygen in simulated gases on the Hg^0 adsorption. The removal efficiency of Hg^0 by the

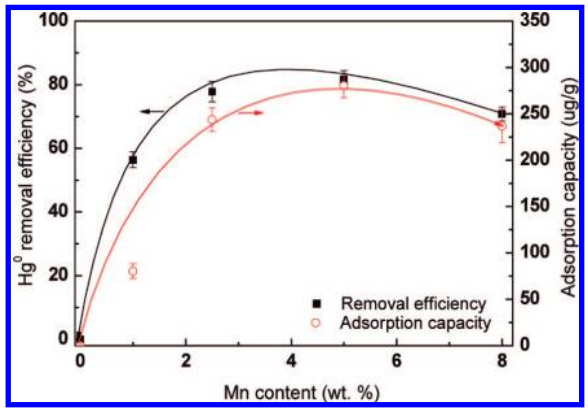

Figure 3. Mn content vs Hg^0 removal efficiency and adsorption capacity at 623 K.The adsorption capacity means the mercury content on the catalysts at 90% breakthrough point of Hg^0, $Q_{90\%}$.

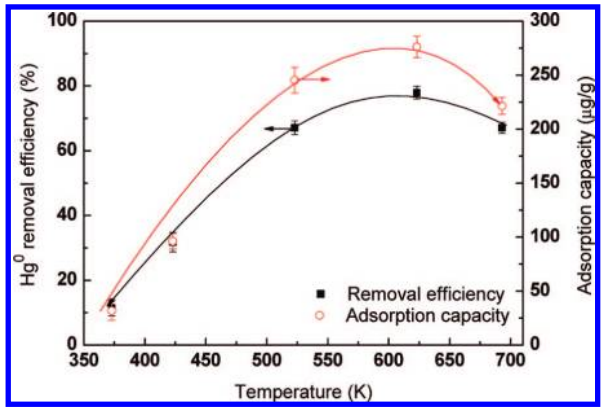

Figure 4. Temperature dependence of the Hg^0 removal efficiency and the adsorption capacity. Mn content on the catalyst was 2.5%.

adsorption of the catalyst in nitrogen (without oxygen) was much lower than that in the air (21% of oxygen), and the adsorption of Hg^0 became negligible after 5 h of adsorption. This indicated that the adsorption of Hg^0 might comprise some chemical reactions with oxygen involved, which will be discussed later. The adsorption of Hg^0 with 5% of oxygen concentration in the gas was slightly lower than that in the air (21% of oxygen), which suggested that oxygen concentration in the common coal-fired flue gases (3−8%) was sufficient to promote the adsorption of Hg^0.

The Effect of Loaded Mn Content on Hg^0 Adsorption. The effects of the Mn content on the Hg^0 removal efficiency and the adsorption capacity ($Q_{90\%}$) at 623 K are shown in Figure 3. It was obvious that the removal efficiency of Hg^0 by adsorption went up as the Mn content on the catalysts increased from 1.0% to 5.0%. The Hg^0 adsorption capacity, $Q_{90\%}$, also increased from 75 μg/g at 1% of loaded Mn to about 270 μg/g at a Mn content of 5%. However, further increase of Mn content from 5% to 8% resulted in a slight drop in both Hg^0 removal efficiency and capacity. The result was attributed to the aggregation of excessive MnO_x loaded on the catalyst surface, which would deteriorate the porosity of the surface. So the optimal Mn content on the catalysts appeared to be about 5%.

Effect of the Temperature on Hg^0 Adsorption. The effect of the temperature on the removal efficiency and adsorption capacity on Hg^0 were tested from 373 to 693 K, and the results are shown in Figure 4. The removal efficiency increased from about 10% to 78% when the temperature rose from 373 to 623 K, and then it dropped to 67% at 693 K. In addition, the adsorption capacity on Hg^0 almost synchronously varied with

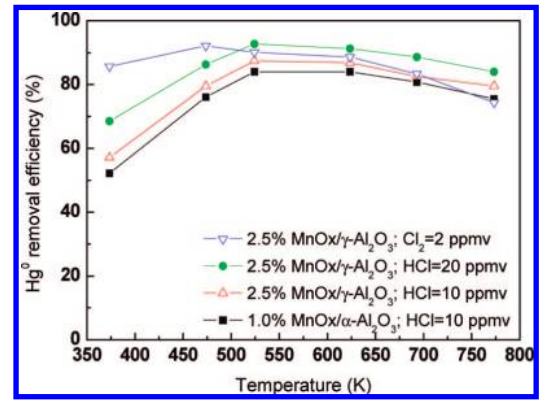

Figure 5. Removal efficiency of Hg^0 in the presence of HCl or Cl_2 under various temperatures.

the removal efficiency and the temperature. Generally, rising temperature would display a negative effect on the physical adsorption, instead of enhancing it. Thus it was evident that the adsorption of Hg^0 on the catalysts was dominated by a certain chemical process.

3.2. Catalytic Oxidation of Hg^0 over the Catalysts in the Presence of HCl or Cl_2. Most coal contains a certain amount of chloride compounds, and HCl would be present in the flue gas when the coals were fired. Therefore, the effect of HCl on the catalytic oxidation of Hg^0 was examined. Figure 5 illustrates the effect of HCl on the oxidation efficiency of Hg^0 at different temperatures and HCl concentrations. In order to minimize the contribution of Hg^0 adsorption on the measured data in catalysis, all the data in the figure was acquired with the following sequences: the gas containing Hg^0 passed through the reactor with catalyst until the Hg^0 adsorption reached 90% breakthrough on the catalyst; then various concentrations of HCl or Cl_2 were added into the gases for about 4 h, and the Hg^0 concentration in the outlet would drop and tend to be constant. Then the data was used to calculate the oxidation efficiency of Hg^0.

It can be seen that the presence of HCl can remarkably increase the Hg^0 oxidation efficiency even when the catalyst has been saturated with the adsorbed mercury under the same conditions. MnO_x/α-alumina catalyst displayed significant catalysis on Hg^0 oxidation in the presence of HCl. This indicated that the catalytic oxidation of Hg^0 was a rapid process on the catalyst surface.

In addition, the higher concentration of HCl utilized in the gas corresponded to the higher oxidation efficiency, and it was about 92% with 20 ppm of HCl in the gas for MnO_x/γ-alumina containing 2.5% Mn. In addition, the effect of the temperature on the catalytic oxidation of Hg^0 was also significant. Increasing the temperature from 373 to 623 K can facilitate the oxidation of Hg^0; then it became flat and dropped slightly when the temperature went up further. The optimal temperature was also around 600 K.

It has been proven that a small amount of Cl_2 can be produced by catalytic oxidation of HCl over catalysts.[15] Therefore, the effect of Cl_2 on the catalytic oxidation of Hg^0 in the presence of the catalyst was also investigated, and the results are also shown in Figure 5 for the purpose of comparison. It can be seen that Cl_2 was more effective on the oxidation of Hg^0 than HCl, and 2 ppm of Cl_2 can achieve almost the same oxidation efficiency of Hg^0 as 20 ppm of HCl. Meanwhile, the temperature dependence of Hg^0 oxidation efficiency with Cl_2 was slightly different from that with HCl, and the optimal temperature was

Table 1. Adsorption and Regeneration of Mercury on the Catalysts[a]

tested conditions	inlet Hg^0 ($\mu g/m^3$)	adsorbed mercury on catalysts ($\mu g/g$)	outlet mercury	
			Hg^0 ($\mu g/m^3$)	Hg^{2+} ($\mu g/m^3$)
MnO_x/γ-Al_2O_3, without HCl, adsorption only; adsorption time, 12 h	180	78.0	48	ND[b]
MnO_x/γ-Al_2O_3, with 20 ppm of HCl without preadsorbed mercury, 2 h	180	2.2	15	147
MnO_x/γ-Al_2O_3, with 100 ppm of HCl with 180 $\mu g/g$ of preadsorbed mercury; HCl treated time, 0.5 h	0	27.5	ND[b]	5500
MnO_x/γ-Al_2O_3, with 100 ppm of HCl with 180 $\mu g/g$ of preadsorbed mercury; HCl treated time, 2 h	0	7.5	ND[b]	180

[a] The gas flow rate was 100 L/h at 623 K. The catalyst was MnO_x/γ-Al_2O_3 with 2.5% Mn content. [b] ND means not detectable.

around 500 K. This indicated that Cl_2 was more easily activated to oxidize Hg^0 at lower temperatures.

Furthermore, the analysis of the mercury adsorption capacity on MnO_x/γ-Al_2O_3 with 2.5% Mn content at 623 K showed that the accumulated adsorbed mercury on the catalysts was very little in the presence of HCl, even though it has been presaturated with Hg^0 (see Table 1). Almost all the adsorbed mercury was converted to $HgCl_2$ and then released into gas phase since $HgCl_2$ is readily vaporized at 373 K or higher. The total mercury (including Hg^{2+} and Hg^0) in the outlet was almost equal to that in the inlet if HCl continued to be present in the gas, with about 90% of the mass balance. Therefore, MnO_x would convert Hg^0 to the oxidized form in the presence of HCl or Cl_2, and the contribution of adsorption to the overall removal efficiency was negligible.

Therefore, MnO_x/γ-alumina was demonstrated to be either the sorbent or the catalyst. The adsorption would play an important role to remove Hg^0 if the flue gas contained less chloride species. Moreover, the catalyst with adsorbed mercury can be regenerated by injecting gaseous HCl or Cl_2 into the reactor. As shown in Table 1, the catalysts with 180 $\mu g/g$ of adsorbed mercury can be effectively regenerated by flushing with 100 ppm of HCl in the gas, and about 80% of the mercury was driven off after 0.5 h of the treatment. The maximum $HgCl_2$ concentration in the effluent gas was up to 5500 $\mu g/m^3$, which was very easily concentrated and recovered by adsorption or absorption methods. The regeneration process can be finished within 2 h. Therefore, this method was more practical than the temperature-swing method, which would consume more energy and might cause the sinter of the catalyst at higher temperature.

3.3. Effects of the Main Components in Flue Gas on the Hg^0 Adsorption and Catalytic Oxidation. The effects of SO_2, NO (400 ppm), CO_2 (2%), and water vapor (0−5%) on the adsorption and conversion of Hg^0 over the catalysts were also investigated at 623 K. No significant effects of NO, CO_2, or water vapor were observed on the removal efficiency of Hg^0 no matter whether HCl was present or not. However, the effect of SO_2 on the adsorption and catalytic oxidation of Hg^0 was remarkable (see Figure 6). Among the tested cases, the removal efficiency of Hg^0 by adsorption only appeared to be very sensitive to SO_2. It dropped dramatically to 57% at 500 ppmv of SO_2, compared with that of 78% without SO_2.

The catalytic conversion of Hg^0 with HCl and Cl_2 was also inhibited in the presence of SO_2, but the degree of inhibition was less than that on the adsorption. With 500 ppm of SO_2 and 20 ppm of HCl in the gas, the removal efficiency of Hg^0 was about 83%, which was about 8% lower than that without SO_2. Similarly, the removal efficiency of Hg^0 at 2 ppm of Cl_2 dropped to 87%, with about 4% reduction in the presence of 500 ppm of SO_2. Relatively, Cl_2 employed to oxidize Hg^0 appeared to be less inhibited by SO_2 compared with HCl.

The inhibition of SO_2 to the adsorption and oxidation of Hg^0 can be tentatively explained as follows. SO_2 would compete against mercury for the activity sites on the catalyst and resulted in the decreased removal efficiency by adsorption. Similarly, the sites used for the activation of HCl or Cl_2 were also competitively occupied by SO_2, which resulted in the lower Hg^0 removal efficiency. Therefore, the inhibition of SO_2 to the catalyst should be minimized by improving the catalyst's property, such as with the method reported in the similar study on SCR catalyst by doping some chemical elements into the catalysts.[16,17]

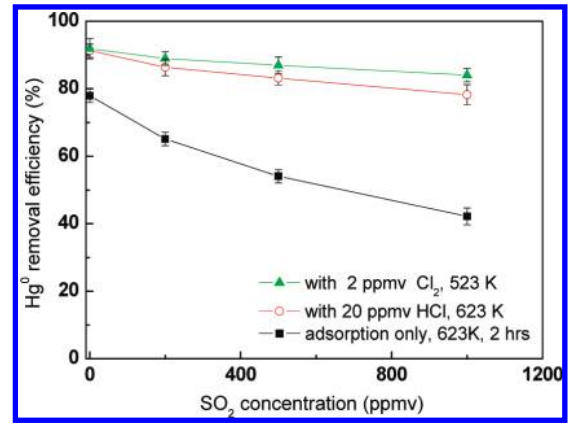

Figure 6. Effect of SO_2 on Hg^0 removal efficiency at various conditions. The catalyst was MnO_x/γ-Al_2O_3 with 2.5% Mn content.

3.4. Determination of the Pathways of Hg^0 Adsorption and Conversion on the Catalysts. Speciation Variation of the Main Elements on the Catalyst. The mechanism and the reaction pathways for Hg^0 adsorption have not been well understood yet. In order to determine the changes of the chemical states of the main elements on catalysts and the speciation of the adsorbed mercury, XPS and pyrolysis−CVAAS techniques were used to analyze the samples with and without the adsorbed mercury.

The XPS spectra of Hg 4f7, O 1s, and Mn 2p on the catalysts with and without adsorbed mercury were scanned, and the results are shown in Figure 7. The Hg 4f7 spectra of the adsorbed mercury on the catalyst ranged from 99 to 104 eV, which indicated that the adsorbed mercury presented as various forms on the catalyst. The spectra can be tentatively divided into two peaks; one was at about 100.8 eV, and the other was at about 100.2 eV. The former peak was determined to be the response of HgO or oxidized mercury (Hg^{2+}), and the latter corresponded to the weakly bonded mercury on the catalyst, which was the complex with the peak between the spectra of elemental mercury (with the peak at about 99.5 eV) and Hg^{2+} (>100.4 eV Hg^0).

For the element Mn, two main peaks due to Mn 2p3/2 and Mn 2p1/2 were observed from 639 to 660 eV. By analysis of the Mn spectra, MnO_x on the catalysts was determined to be present mainly in the states of Mn(IV) and Mn(III), with the corresponding binding energy at 643.7 and 641.9 eV, respec-

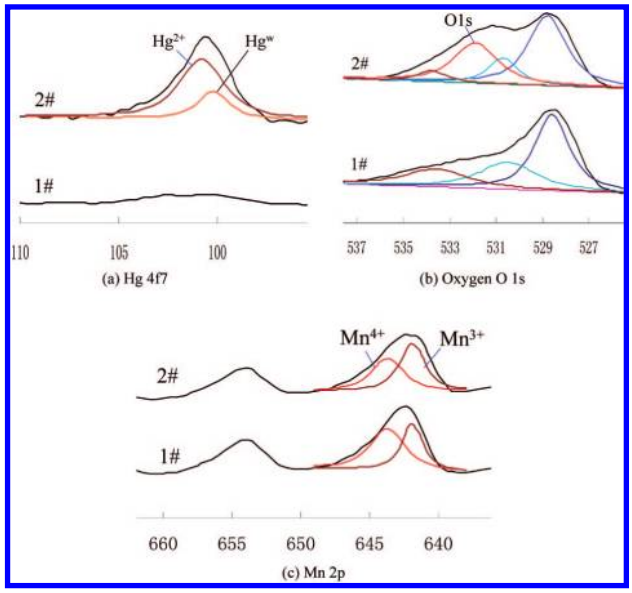

Figure 7. XPS spectra of Hg, Mn, and oxygen with and without the adsorbed mercury: 1#, 2.5% MnO_x/γ-Al_2O_3 without adsorbed mercury; 2# 2.5% MnO_x/γ-Al_2O_3 with 78 μg/g of adsorbed mercury; Hg^w denotes the weakly bonded mercury.

tively.[16] The ratio of the spectra area with respect to Mn(III) and Mn(IV) was about 0.92 for the blank catalyst without mercury, but the ratio increased to 1.2 as 78 μg/g of mercury was adsorbed on the catalyst. It indicated that some of the Mn(IV) was converted to Mn(III) by reacting with Hg^0 during the adsorption process.

The XPS spectra of O 1s on the catalysts are shown in Figure 7b. Generally, various oxygen species on the catalyst corresponded to the respective bonding energy values, and the different types of O 1s peaks can be judged from the difference in the electronegativity of the elements. The peak at 529.6−530.0 eV corresponds to lattice oxygen (O^{2-}), and the peak in the region of 531.7 eV corresponds to the weakly adsorbed species oxygen state (O^-). The peaks at 530.5 and 532.6 eV represent the −Mn-OH and H_2O molecules, respectively. It can be observed that the peak at 531.7 eV went up after the catalyst adsorbed enough mercury. Taking into account the peak of Hg 4f7 at 100.2 eV, it was supposed that the weakly adsorbed mercury on the catalysts might be bonded with these weakly adsorbed species O-oxygen.

In addition, the pyrolysis−CVAAS patterns of the samples are shown in Figure 8. It was found that two peaks with different retention time appeared in the pyrolysis−AAS patterns of the adsorbed mercury. According to the decomposition sequences of different mercury species, the first peak was determined to be the weakly bonded mercury, and the latter was the stronger bonded mercury. In order to determine the two mercury species on the catalysts, the samples with the adsorbed mercury were treated by soaking with 1 mol/L nitric acid solution and followed by washing and dryness, and then the samples were analyzed again. It was found that nitric acid solution can efficiently dissolve the mercury speciation corresponding to the latter peak, but the speciation with respect to the former peak was difficult to be dissolved. Therefore, the latter peak represented HgO or oxidized mercury, which was determined from its chemical property. The analysis results by pyrolysis−AAS were consistent with the XPS results.

Additionally, it can be found that the ratios of the peak area of the weakly bonded speciation to HgO also varied, and it went up with the rise of the adsorbed mercury amount on the catalyst.

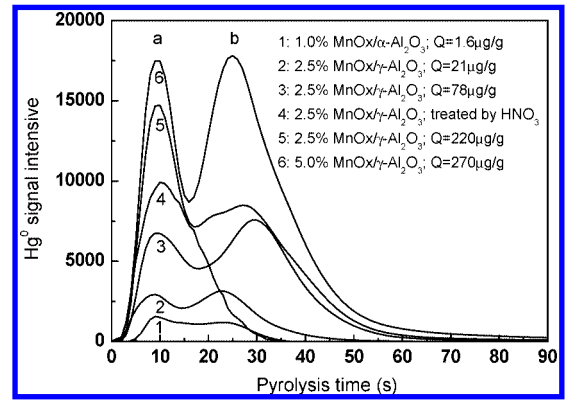

Figure 8. Pyrolysis−AAS patterns of mercury from various catalysts with adsorbed mercury: (a) weakly bonded mercury; (b) HgO or the oxidized mercury. The amount of the pyrolyzed samples in every test ranged from 5 to 15 mg.

For the catalyst MnO_x/γ-Al_2O_3 with 2.5% Mn, about 23% of the absorbed mercury was in the weakly bonded form when the total adsorbed amount was 78 μg/g at 623 K, but it increased to 46% as the adsorbed amount was 220 μg/g. It was also observed from Figure 8 that the ratio of the weakly bonded speciation to HgO decreases with the increased Mn content on the catalysts if the same content of mercury was adsorbed.

Mechanism for Hg^0 Adsorption and Conversion. From the above results, the adsorption mechanism can be explained by the Mars−Maessen mechanism.[18] First, the gaseous Hg^0 was adsorbed on the catalyst by the physical adsorption to form $Hg^0_{(ad)}$; then $Hg^0_{(ad)}$ will be further converted through two pathways: one is that $Hg^0_{(ad)}$ will bond with the lattice oxygen on the catalyst to form the weakly bonded speciation Hg−O−Mn−O_{x-1}, and the other is that $Hg^0_{(ad)}$ would abstract a lattice oxygen to form HgO directly. The uptake of the lattice oxygen by mercury over the catalyst will be compensated by activating the gaseous oxygen from the gas.

$$Hg^0(g) \rightarrow Hg^0_{(ad)} \quad (2)$$

$$Hg^0_{(ad)} + MnO_x \rightarrow Hg{-}O{-}MnO_{x-1} \quad (3)$$

$$Hg^0_{(ad)} + MnO_x \rightarrow HgO + MnO_{x-1} \quad (4)$$

$$Hg{-}O{-}MnO_{x-1} \rightarrow HgO + MnO_{x-1} \quad (5)$$

$$MnO_{x-1} + 1/2O_2 \rightarrow MnO_x \quad (6)$$

where Hg−O−MnO_{x-1} represents the weakly bonded speciation.

The adsorption processes of Hg^0 over the catalysts were considered to be controlled by both thermodynamic equilibrium and reaction kinetics. Generally, the lower temperature will facilitate the physical adsorption step from $Hg^0_{(g)}$ to $Hg^0_{(ad)}$. But the conversion of $Hg^0_{(ad)}$ to the weakly bonded mercury or HgO was the chemical steps, and increasing temperature will help accelerate the reaction rate.

The mechanism for the catalytic conversion of Hg^0 in the presence of HCl has been tentatively proposed by various pathways, among which the Deacon process is well accepted.[15] In the presence of an appropriate catalyst and favorable temperature range, part of the HCl in the flue gas could be catalytically converted to active chlorine atom (Cl) or chlorine molecule (Cl_2) on the catalyst, which thereby enhances the oxidation of Hg^0. The proposed processes can be described as follows

$$HCl + \otimes \rightarrow H + Cl\otimes \quad (7)$$

$$Cl\otimes + Cl\otimes \rightarrow Cl_2 + 2\otimes \quad (8)$$

$$Hg + Cl \rightarrow HgCl \quad (9)$$

$$HgCl + Cl \rightarrow HgCl_2 \quad (10\text{-a})$$

$$HgCl + HCl \rightarrow HgCl_2 + H \quad (10\text{-b})$$

$$HgCl + Cl_2 \rightarrow HgCl_2 + Cl \quad (10\text{-c})$$

in which $\otimes$ represents the available active sites on MnO_x catalyst surface.

Consequently, the reactions involved in the oxidation of mercury could be expressed with eqs 7−10-c. The reactions between Hg^0 and HCl over the catalyst were considered to be consistent with the Langmuir−Hinshelwood mechanism, where the reaction occurred among the adsorbed species on the surface of the catalyst. Meanwhile, the reaction between Hg^0 and Cl_2 was similar to that for HCl, but the activation of Cl_2 was relatively easier. Therefore, the favorable temperature range with Cl_2 was lower than that with HCl.

4. Conclusions

The MnO_x/alumina catalyst, manganese oxide impregnated on alumina, can remove Hg^0 from flue gas by both adsorption and catalytic oxidation. The adsorption played an important role in the absence of HCl, and the favorable adsorption temperature was about 600 K. However, the catalytic oxidation of elemental mercury became dominant when HCl or Cl_2 was present in the flue gas. Over 90% of Hg^0 can be obtained with 20 ppm of HCl or 2 ppm of Cl_2. In addition, the catalysts with adsorbed mercury can be chemically regenerated by rinsing with HCl gas to strip off the adsorbed mercury in the form of $HgCl_2$. SO_2 displayed inhibition to the adsorption of Hg^0 on the catalyst, but the inhibition was less to the catalytic oxidation of Hg^0, especially in the presence of Cl_2. The analysis results of XPS and pyrolysis−AAS indicated that the adsorbed mercury was mainly in the form of HgO and the weakly bonded speciation Hg−O−MnO_{x-1}, and the ratio of them varied with the adsorption amount and the content of MnO_x. The adsorption and catalytic oxidation performances of MnO_x/Al_2O_3 on Hg^0 appeared to promote its application in industry.

Acknowledgment

This study was supported by the High-Tech R&D Program of China (863) under Grant No. 2007AA06Z340.

Literature Cited

(1) Granite, E. J.; Myers, C R.; King, W. P.; Stanko, D. C.; Pennline, H. W. Sorbents for mercury capture from fuel gas with application to gasification systems. *Ind. Eng. Chem. Res.* **2006**, *45*, 4844.

(2) United Nations Environment Programme (UNEP), Global Mercury Assessment, UNEP Chemicals, Geneva, Switzerland, Dec. 2002.

(3) Wu, Y.; Wang, S. X.; Streets, D. G.; Hao, J. M.; Chao, M.; Jiang, J. K. Trends in anthropogenic mercury emissions in China from 1995 to 2003. *Environ. Sci. Technol.* **2006**, *40*, 5312.

(4) Jiang, G. B.; Shi, J. B.; Feng, X. B. Mercury pollution in China. *Environ. Sci. Technol.* **2006**, *40*, 3673.

(5) John, H. P.; Everett, A. S.; Michael, D. M. Status review of mercury control options for coal-fired power plants. *Fuel Process. Technol.* **2003**, *82*, 89.

(6) Strivastava, R. K.; Hutson, N.; Princiotta, F.; Straudt, J. Control of mercury emission from coal-fired electric utility boilers. *Environ. Sci. Technol.* **2006**, *40*, 2385.

(7) Yan, N. Q.; Liu, S. H.; Miller, C.; Chang, S. G. Method for the study of gaseous oxidants for the oxidation of mercury gas. *Ind. Eng. Chem. Res.* **2005**, *44*, 5567.

(8) Kilgroe, J.; Senior, C. Fundamental science and engineering of mercury control in coal-fired power plants. *Proceedings of Air Quality IV*, *International Conference on Mercury, Trace Elements, and Particulate Matter*, Arlington, VA, Sept. 22−24, 2003.

(9) Cao, Y.; Chen, B.; Wu, J. S.; Cui, H.; Smith, J.; Chen, C. K.; Chu, P.; Pan, W. P. Study of mercury oxidation by a selective catalytic reduction catalyst in a pilot-scale slipstream reactor at a utility boiler burning bituminous coal. *Energy Fuels* **2007**, *21*, 145.

(10) Chu, P.; Laudal, D. L.; Brickett, L.; Lee, C. W. Power plant evaluation of the effect of SCR technology on mercury. *Proceedings of the Combined Power Plant Air Pollutant Control Symposium−The Mega Symposium*, Washington, DC, May 19−22, 2003.

(11) Cao, Y.; Gao, Z. Y.; Zhu, J. S.; Wu, Q. H.; Huang, Y. J.; Chiu, C. C.; Parker, B.; Chu, P.; Pan, W. P. Impacts of halogen additions on mercury oxidation, in a slipstream selective catalyst reduction (SCR) reactor when burning sub-bituminous coal. *Environ. Sci. Technol.* **2008**, *42*, 256.

(12) Li, J.; Chen, J.; Ke, R.; Luo, C.; Hao, J. Effects of precursors on the surface Mn species and the activities for NO reduction over $MnOx/TiO_2$ catalysts. *Catal. Commun.* **2007**, *8*, 1896.

(13) Wu, Z. B.; Jiang, B. Q.; Liu, Y.; Zhao, W. R.; Guan, B. H. Experimental study on a low-temperature SCR catalyst based on $MnOx/TiO_2$ prepared by sol-gel method. *J. Hazard. Mater.* **2007**, *145*, 488.

(14) Qi, G. S.; Yang, R. T.; Chang, R. $MnOx-CeO_2$ mixed oxides prepared by co-precipitation for selective catalytic reduction of NO with NH_3 at low temperatures. *Appl. Catal., B* **2004**, *51*, 93.

(15) Pan, H.; Minet, R.; Benson, S.; Tsotsis, T. Process for converting hydrogen chloride to chlorine. *Ind. Eng. Chem. Res.* **1994**, *33*, 2996.

(16) Wu, Z. B.; Jiang, B. Q.; Liu, Y. Effect of transition metals addition on the catalyst of manganese/titania for low-temperature selective catalytic reduction of nitric oxide with ammonia. *Appl. Catal., B* **2008**, *79*, 347.

(17) Wu, Z. B.; Jiang, B. Q.; Liu, Y.; Wang, H. Q.; Jin, R. Drift study of manganese/titania-based catalysts for low-temperature selective catalytic reduction of NO with NH_3. *Environ. Sci. Technol.* **2007**, *41*, 5812–5817.

(18) Granite, E. J.; Pennline, H. W.; Hargis, R. A. Novel sorbents for mercury removal from flue gas. *Ind. Eng. Chem. Res.* **2000**, *39*, 1020.

Received for review October 1, 2008
Revised manuscript received January 20, 2009
Accepted January 22, 2009

IE801478W